A new trajectory tracking controller for the unicycle mobile robot

I. Estrada-Sánchez, M. Velasco-Villa, and H. Rodríguez-Cortés

Sección de Mecatrónica, Departamento de Ingeniería Eléctrica, Centro de Investigación y de Estudios Avanzados del Instituto Politécnico Nacional, México City, México, (emails:{ivanestrada,velasco,hrodriguez}@cinvestav.mx)

Abstract: This work proposes a robust geometric controller to solve the trajectory tracking problem for unicycle mobile robot. The proposed control design exploits the cascade structure of the unicycle translational and rotational kinematics. An estimator endows the proposed controller with the capability to actively reject constant translational disturbances. Numerical simulation results show the performance of the proposed control algorithm.

Keywords: Geometric control, translational and rotational kinematics, nonlinear estimators, cascade structure, disturbance rejection.

1. INTRODUCTION

The number and complexity of applications of mobile robots in daily life are increasing. Current research focuses on the integration of new sensors, the development of collaborative protocols, and the communication through the internet. Internet of things opens a new world of applications for mobile robots. At the core of all these new demands, a low-level controller runs to ensure that mobile robots perform as dictated by high-level maker decisions. Since unicycle mobile robots are underactuated, nonlinear and satisfy nonholonomic constraints, low-level control design to solve the regulation and trajectory tracking problems is an active area of research. The unicycle kinematic model falls among the class of nonlinear systems for which do not exists a continuous state feedback control rendering the origin asymptotically stable, Brockett (1983). Additionally, the unicycle attitude has a nonlinear configuration space, this is, the unit circle. As the unit circle is not diffeomorphic to the one-dimensional Euclidean space, it is not possible to achieve global asymptotic stability with a continuous state feedback, Bhat and Bernstein (2000).

To go around the topological constraints to stabilize the unicycle posture, researchers proposed the following solutions using continuous controllers. The first approach selects a suitable reference trajectory; then it is possible to stabilize the unicycle posture around the selected reference, Jiang and Nijmeyer (1997). The second solution defines new outputs to command. These outputs link the unicycle Cartesian position with the unicycle attitude; it turns out that the unicycle kinematics becomes input-output linearizable, Morin and Samson (2008), Rouchon et al. (1993). A third approach suggests changing the unicycle coordinates to polar coordinates Astolfi (1999) or Frenet frame coordinates Morin and Samson (2008). A fourth approach linearizes the unicycle kinematics dynamically Oriolo et al. (2002). Some other solutions propose time varying and discontinuous controllers, for instance Maghenem et al. (2016), Buccieri et al. (2009).

Most of the proposed controllers focus on tackling the topological constraint imposed by the nonholonomic characteristic of the unicycle kinematics. The limitation to achieving global stability because of the nonlinear configuration space of the unicycle attitude has attracted less attention, and it is common to use local attitude coordinates for control design. Using local coordinates turns out to be double-valued on the unit circle, as a consequence the closed-loop dynamics exhibits the unwinding phenomena, Bhat and Bernstein (2000). Additionally, a Lyapunov-based proof for global stability requires a radially unbounded Lyapunov function. Radial unboundedness is not achievable for the unicycle attitude as it lives on the unit circle.

The limitations to achieve global asymptotic stability with time-invariant continuous controllers in mechanical systems with configuration spaces non-homeomorphic to the Euclidean space where pointed out in Koditschek (1989). The unwinding phenomena consequence of control design using local coordinates described in Bhat and Bernstein (2000) led to the development of new control strategies directly on the nonlinear configuration space Chaturvedi et al. (2011), McClamroch et al. (2017), Maithripala and Berg (2015).

This article proposes a trajectory tracking controller for the unicycle mobile robot considering the nonlinear configuration space of the unicycle attitude. Control design profits of the cascade interconnection between the translational and rotational unicycle kinematics. This cascade interconnection is pointed out in Lee et al. (2013) for the quadrotor vehicle. A disturbance estimator, based on the Immersion and Invariance method Astolfi et al. (2007), endows the proposed controller with the ability to actively reject constant bounded disturbances acting on

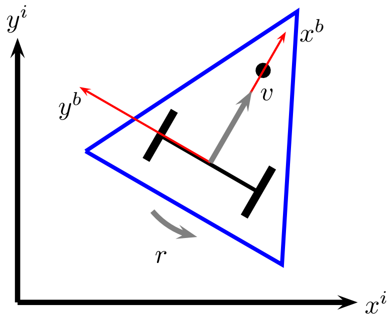

Fig. 1. Mobile robot, z^i and z^b point out of the drawing.

the translational kinematics. Numerical simulations show the performance of the proposed control scheme.

The organization of this document is as follows. Section 2 presents the kinematic model and points out the cascade interconnection between the translational and rotational kinematics. Section 3 describes the developments to design the controller and the disturbance estimator, as well as, the stability analysis. Section 4 shows the numerical simulations of the closed-loop dynamics. Finally, Section 5 provides some concluding remarks.

2. KINEMATIC MODEL

Two coordinate frames are needed to define the mobile robot kinematics; the inertial coordinate frame $x^i y^i z^i$ and the body coordinate frame $x^b y^b z^b$, see Figure (1). The following set of differential equations describes the kinematic model of the mobile robot, Zhang et al. (1998)

$$\begin{aligned} \dot{X} &= vR_2e_1 + \delta \\ \dot{R}_2 &= R_2\hat{r} \end{aligned} \tag{1}$$

where $X = [\,x\ y\,]^\top$ is the Cartesian position of the wheel axis center, v is the mobile robot forward speed, and r is the rotational speed around the z^i axis. Moreover,

$$e_1 = \begin{bmatrix} 1 \\ 0 \end{bmatrix},\ R_2 = \begin{bmatrix} r_{11} & r_{12} \\ -r_{12} & r_{11} \end{bmatrix}$$

with

$$R_2 \in SO(2) = \left\{ R_2 \in \mathbb{R}^{2\times 2} | R_2^\top R_2 = I_2, \det(R_2) = 1 \right\}$$

the rotation matrix from the inertial coordinate frame to the body coordinate frame; I_2 is the 2×2 identity matrix.

The mapping $\hat{(\cdot)} : \mathbb{R} \to \mathrm{so}(2)$ with so(2) the Lie Algebra of $SO(2)$ composed of the 2×2 skew symmetric matrices, thus,

$$\hat{r} = \begin{bmatrix} 0 & -r \\ r & 0 \end{bmatrix}$$

Finally, δ is a disturbance acting on the translational kinematics.

Assumption 1. The disturbance δ and its first time derivative $\dot{\delta}$ are continuous and satisfy

$$\mu = \sup_{t>0} \|\ddot{\delta}\|$$

with μ a positive constant.

Assumption 1 is a common condition for mismatched disturbances, see for example Ginoya et al. (2014), Yang et al. (2013).

In the following, v and r are the control inputs.

The work in Lee et al. (2013) describes the cascade interconnection between the translational dynamics and the rotational kinematics for a quadrotor vehicle. Here, the change of coordinates employed in Lee et al. (2013) is used to point out the cascade interconnection between translational and rotational kinematics. For, note that the translational kinematics can be written as follows

$$\dot{X} = vR_2e_1 \left(\frac{e_1^\top R_{2d}^\top R_2 e_1}{e_1^\top R_{2d}^\top R_2 e_1} \right) \pm \frac{vR_{2d}e_1}{e_1^\top R_{2d}^\top R_2 e_1} + \delta$$

where R_{2d} is the desired rotation matrix. Then, it follows that

$$\dot{X} = \frac{vR_{2d}e_1}{e_1^\top R_{2d}^\top R_2 e_1} + \Psi(R_2, R_{2d}, v) + \delta$$

with

$$\Psi(R_2, R_{2d}, v) = \frac{v}{e_1^\top R_{2d}^\top R_2 e_1} \left[\left(e_1^\top R_{2d}^\top R_2 e_1 \right) R_2 e_1 - R_{2d} e_1 \right] \tag{2}$$

Now, by defining

$$v = u^\top R_2 e_1,\ R_{2d}e_1 = \frac{u}{\|u\|} \tag{3}$$

with $u = [\,u_x\ u_y\,]^\top$ a new control input and $\|\cdot\|$ the Euclidean norm, one has

$$\begin{aligned} \dot{X} &= u + \Psi(R_2, R_{2d}, v) + \delta \\ \dot{R}_2 &= R_2\hat{r} \end{aligned} \tag{4}$$

Equation (4) exposes the cascade interconnection between the translational and rotational kinematics. Note that, the convergence of the rotation matrix to the desired rotation matrix implies that Ψ converges to zero.

3. CONTROLLER DESIGN AND DISTURBANCE ESTIMATOR

At this point, it is possible to state the control objective. Design control inputs u and r such that the Cartesian position of the wheel axis center converges to a differentiable desired position, while actively compensating the effect of the disturbance.

First, the disturbance estimator is designed as follows. Define the following estimation errors, Astolfi et al. (2007)

$$\begin{aligned} z_1 &= \delta - \eta_1 + \beta_1(X) \\ z_2 &= \dot{\delta} - \eta_2 + \beta_2(X) \end{aligned} \tag{5}$$

Note that

$$\begin{aligned} \lim_{t\to\infty} z_1 = 0 &\Rightarrow \lim_{t\to\infty} (\eta_1 - \beta_1) = \delta \\ \lim_{t\to\infty} z_2 = 0 &\Rightarrow \lim_{t\to\infty} (\eta_2 - \beta_2) = \dot{\delta} \end{aligned}$$

thus; the estimator design objective is to define the dynamics of η_1 and η_2 in such a way that the estimation errors z_1 and z_2 asymptotically converge to zero.

Defining

$$\begin{aligned} \dot{\eta}_1 &= \eta_2 - \beta_2 + \frac{\partial \beta_1}{\partial X}(vR_2e_1 + \eta_1 - \beta_1) \\ \dot{\eta}_2 &= \frac{\partial \beta_2}{\partial X}(vR_2e_1 + \eta_1 - \beta_1) \end{aligned} \tag{6}$$

one obtains

$$\dot{Z} = A_Z Z + B_Z \ddot{\delta} \tag{7}$$

where

$$Z = \begin{bmatrix} z_1 \\ z_2 \end{bmatrix},\ A_Z = \begin{bmatrix} -\Gamma_1 & I_2 \\ -\Gamma_2 & 0_2 \end{bmatrix},\ B_Z = \begin{bmatrix} 0_2 \\ I_2 \end{bmatrix}$$

$$\frac{\partial \beta_1}{\partial X} = -\Gamma_1,\ \frac{\partial \beta_2}{\partial X} = -\Gamma_2$$

with Γ_1 and Γ_2 positive definite matrices and 0_2 is a 2×2 matrix with zero elements.

Proposition 2. Consider that Assumption 1 holds and assume that there exist Γ_1 and Γ_2 such that A_Z is a Hurwitz matrix. Then, the estimation error dynamics is input to state stable.

Proof. Conditions of Lemma 4.6 of Khalil (2002) are satisfied with

$$V_Z = Z^\top P_Z Z, \text{ with, } A_Z^\top P_Z + P_Z A_Z = -I_4$$

where I_4 is a 4×4 identity matrix, and

$$\dot{V}_Z \leq -(1-\theta)\|Z\|^2, \; \forall \, \|Z\| \geq \frac{2\lambda_M(P_Z)}{\theta}\|\ddot{\delta}\|$$

$0<\theta<1$, $\lambda_M(P_Z)$ the largest eigenvalue of P_Z.

Now, the proposed controller is described. Consider a continuous desired translational trajectory denoted by X_d. The tracking error is

$$\tilde{X} = X - X_d$$

From equation (4), the virtual control input u is defined as

$$u = -K_P\tilde{X} - (\eta_1 - \beta_1(X)) + \dot{X}_d \tag{8}$$

The term $\eta_1 - \beta_1(X)$ compensates the action of δ. From equation (3) it is noticed that the definition of u fixes the control input v and the first column of the desired rotation matrix R_{2d}.

The desired matrix R_{2d} must be orthonormal. This can be achieved by defining

$$R_{2d} = \frac{1}{\|u\|}\left[\, u \;\; \hat{1}u \,\right]$$

The distance between R_2 and R_{2d} can be measured from the navigation function defined as, Koditschek (1989), Lee et al. (2013),

$$\varphi(\tilde{R}_2) = \mathrm{tr}\left(I_2 - \tilde{R}_2\right) \tag{9}$$

with $\mathrm{tr}(\cdot)$ is the trace of $(\cdot)$ and $\tilde{R}_2 = R_{2d}^\top R_2$. The navigation function has a local minimum at $\tilde{R}_2 = I_2$, Koditschek (1989).

The error between R_2 and R_{2d} is computed from the gradient of the navigation function. The gradient of the navigation function is given as

$$d\varphi = \frac{1}{2}\left(\tilde{R}_2 - \tilde{R}_2^\top\right)^\vee = e_R$$

with $(\cdot)^\vee : \mathrm{so}(2) \to \mathbb{R}$ the inverse of the map $\hat{(\cdot)}$. Moreover,

$$\dot{e}_R = \frac{1}{2}\mathrm{tr}(\tilde{R}_2)\tilde{r}$$

where

$$\tilde{r} = r - r_d \tag{10}$$

and

$$r_d = \left(R_{2d}^\top \dot{R}_{2d}\right)^\vee$$

From equation (10) the control input r is defined as follows

$$r = r_d - \frac{k_r}{2}\frac{\mathrm{tr}(\tilde{R}_2)}{1+\mathrm{tr}(\tilde{R}_2)^2}e_R \tag{11}$$

with k_r is a positive gain.

Even when the observer (6) can deal with time varying disturbances, to show formally the convergence of the tracking error of the closed–loop system (1)–(8)–(11), Assumption 1 will be relaxed to ask δ to be a bounded constant disturbance. As a result, the estimator error dynamics reduces to the following equation

$$\dot{z}_1 = -\Gamma_1 z_1 \tag{12}$$

Additionally, note that using (3) and the fact that $\tilde{R}_2 \in SO(2)$, the term (2) can be written as follows

$$\Psi = \|u\|\left(\sqrt{1-e_R^2}R_2e_1 - R_2\varphi(e_R)\right),$$

$$\varphi(e_R) = \begin{bmatrix} \sqrt{1-e_R^2} \\ -e_R \end{bmatrix}$$

thus; the following equations describe the mobile robot kinematic model in closed-loop with the control inputs (8)-(11) and the disturbance estimator (6)

$$\begin{aligned} \dot{\tilde{X}} &= -K_P\tilde{X} + \|u\|\left(\sqrt{1-e_R^2}R_2e_1 - R_2\varphi(e_R)\right) + z_1 \\ \dot{e}_R &= -\frac{k_r}{2}\frac{\mathrm{tr}(\tilde{R}_2)^2}{1+\mathrm{tr}(\tilde{R}_2)^2}e_R - \frac{1}{\|u\|^2}z_1^\top\left(\Gamma_1 + K_P\right)\widehat{-1}u \\ \dot{z}_1 &= -\Gamma_1 z_1 \end{aligned} \tag{13}$$

Assumption 3. The constant disturbance satisfies

$$\|\delta\| \leq \mu_1$$

with μ_1 a positive constant. The time derivative of the desired trajectory is bounded, this is,

$$\mu_2 \leq \|\dot{X}_d\| \leq \mu_3$$

with μ_2 and μ_3 positive constants.

Now, the solution to the tracking problem is stated as follows.

Proposition 4. Consider Assumption 3 holds. Assume that $\|u\| \neq 0$. Then, the closed-loop dynamics (13) is asymptotically stable.

Proof. The proof of this result is based on standard results on stability of cascade systems. First, consider the cascade composed of the first two equations of (13) with $z_1 = 0$, this is,

$$\begin{aligned} \dot{\tilde{X}} &= -K_P\tilde{X} + \|u\|\left(\sqrt{1-e_R^2}R_2e_1 - R_2\varphi(e_R)\right) \\ \dot{e}_R &= -\frac{k_r}{2}\frac{\mathrm{tr}(\tilde{R}_2)^2}{1+\mathrm{tr}(\tilde{R}_2)^2}e_R \end{aligned} \tag{14}$$

It is clear that $\dot{\tilde{X}} = -K_P\tilde{X}$ is asymptotically stable. Since, $\|u\| \neq 0$ implies that $\mathrm{tr}(\tilde{R}_2) \neq 0$, the e_R dynamics is asymptotically stable. Moreover, $e_R = 0$ implies that

$$\|u\|\left(\sqrt{1-e_R^2}R_2e_1 - R_2\varphi(e_R)\right) = \|u\|\left(R_2e_1 - R_2e_1\right) = 0$$

Hence, by Proposition 4.1 of Sepulchre et al. (1997), the dynamics (14) is asymptotically stable. Asymptotic stability of the closed-loop dynamics (13) follows as a result of asymptotic stability of (14) and $\dot{z}_1 = -\Gamma z_1$, and Proposition 4.1 of Sepulchre et al. (1997).

4. NUMERICAL SIMULATION

To show the operation of the proposed control algorithm, numerical simulations were performed. To show the potentially of the proposed solution, the disturbance is modeled as a time varying signal as follows

$$\delta = |v|\begin{bmatrix} \delta_x & 0 \\ 0 & \delta_y \end{bmatrix} R_2e_2$$

with $\delta_x = 0.1$ and $\delta_y = 0.1$. Thus, the disturbance is equal zero when the mobile robot stops. Notice that this disturbance can be handled by the observer but is not allowed in the proof of the tracking convergence.

The first simulation that was carried out is the trajectory tracking of a square of $4.5\ m \times 4.5\ m$. The desired trajectory was created as described in Table 1. Notice also that this trajectory imposes an additional restriction since it is not differentiable at the corners.

Time	Desired trajectory X_d
$0 < t \le 30$	$X_d = [At, 0]^\top$
$30 < t \le 60$	$X_d = [30A, A(t-30)]^\top$
$60 < t \le 90$	$X_d = [A(90-t), 30A]^\top$
$90 < t \le 120$	$X_d = [0, A(120-t)]^\top$

Table 1. Desired trajectory to track a square with $A = 0.15$

The initial conditions were selected as $X(0) = [0, 0]^\top$ and

$$R_2(0) = \begin{bmatrix} 0.5 & -0.8660 \\ 0.8660 & 0.5 \end{bmatrix}$$

The gains for the estimator were selected as $\Gamma_1 = \text{diag}\{0.5\}$ and $\Gamma_2 = \text{diag}\{0.0625\}$. This gain selection placed the estimator poles at $\{-0.25\}$. The gain of the control input u is $K_P = \text{diag}\{0.7\}$ and the gain for the control input r is $k_r = 2.5$.

Figure 2 shows the translational trajectory tracking errors, as can be seen, they converge to zero. Figure 3 presents the convergence of the attitude error $e_R(t)$ to zero.

Figure 4 presents the control signals r, v applied to the system. The Cartesian trajectory described by the mobile robot is shown in Figure 5.

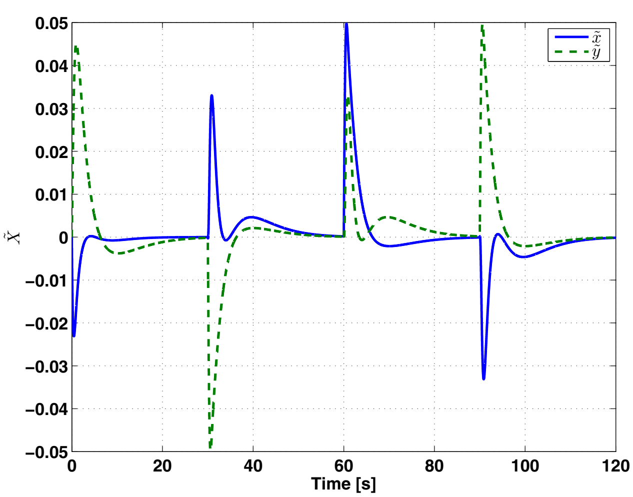

Fig. 2. Trajectory tracking errors $\tilde{X}$.

Finally, Figure 6 shows the behavior of the estimated disturbance.

For the second simulation, a parabolic trajectory was tracked. The initial conditions and control gains were the

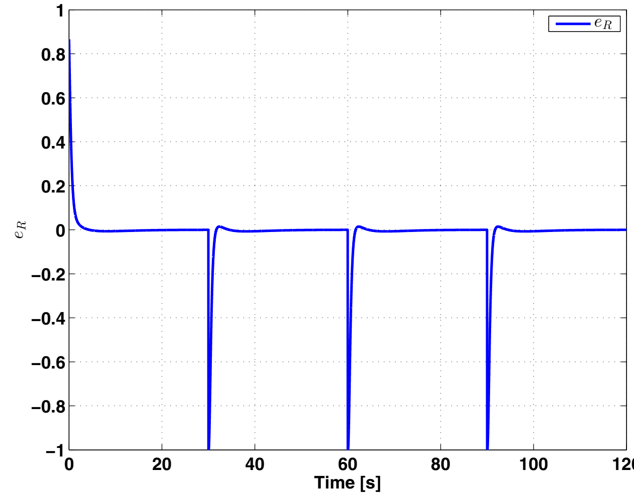

Fig. 3. Attitude error e_R.

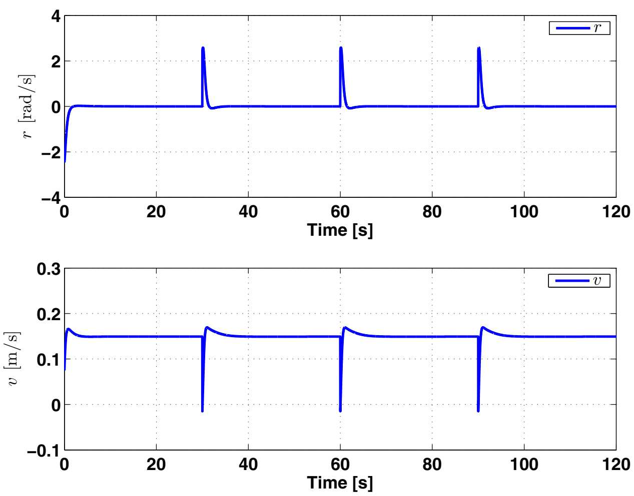

Fig. 4. Control signals r and v.

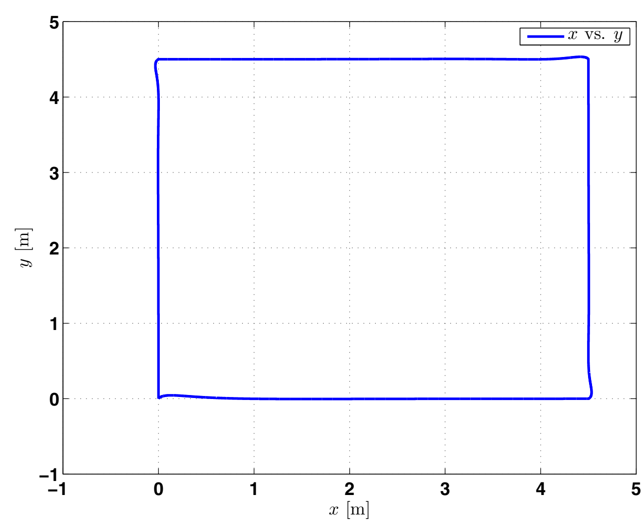

Fig. 5. Path followed by the mobile robot.

same as those used in the first simulation. The desired trajectory was constructed as described in Table 2.

The evolution of the state $X(t)$ in the Cartesian plane is depicted in Figure 7. In Figure 8, the trajectory tracking errors are shown and as it can be observed they converge

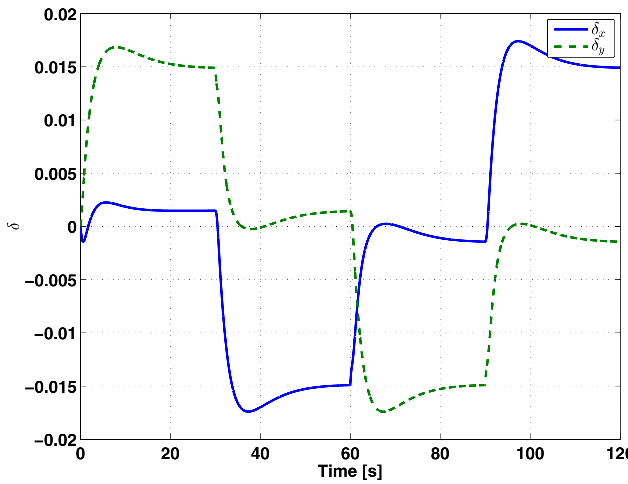

Fig. 6. Estimated disturbance $\eta_1 - \beta_1$.

Time	Desired trajectory X_d
$0 < t \leq 50$	$X_d = [At, Bt^2]^\top$
$t > 50$	$X_d = [100A - At, B\,(100 - t)^2]^\top$

Table 2. Desired reference to track a parabola with $A = 0.05$ and $B = 0.001$

to zero. Figure 9 shows the convergence of the attitude

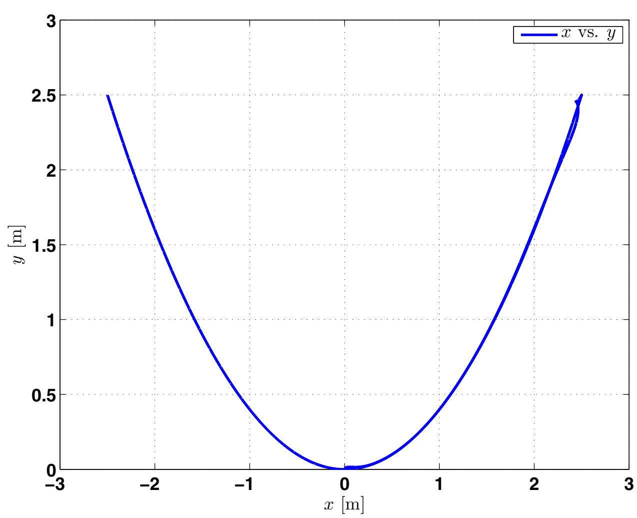

Fig. 7. Path followed by the mobile robot.

error. Figure 10 shows the control signals r, v applied to the system.

Finally, in Figure 11, the estimated disturbance is presented.

5. CONCLUSIONS

This paper proposed a new trajectory tracking controller for the unicycle mobile robot. The proposed controller actively compensates constant disturbances. The theoretical developments are validated by means of numerical simulations. As future work, the control-observation scheme will be implemented in an experimental platform.

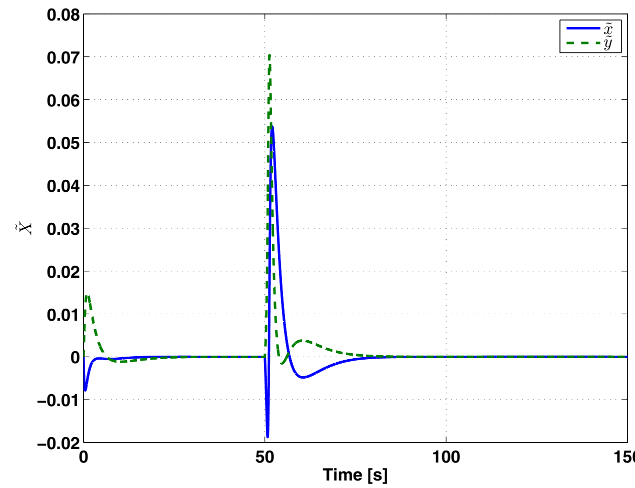

Fig. 8. Trajectory tracking errors $\tilde{X}$.

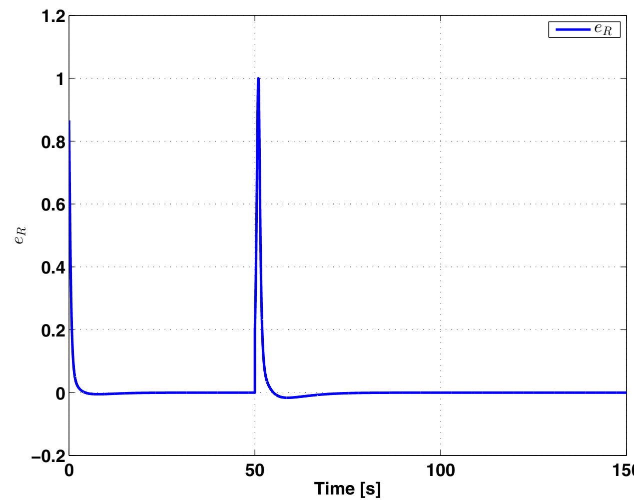

Fig. 9. Orientation error e_R.

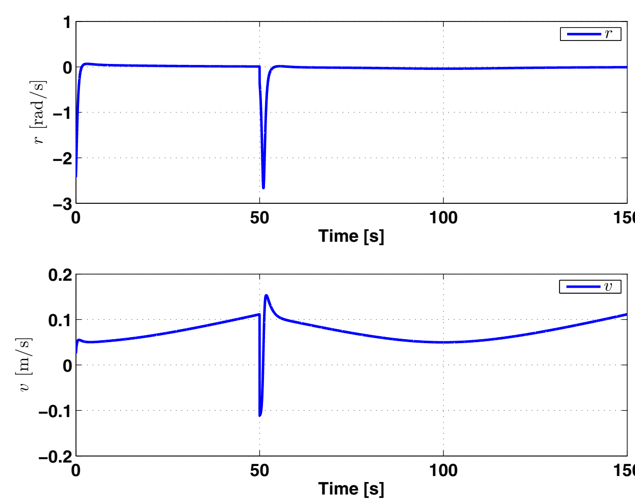

Fig. 10. Control signals r and v.

6. ACKNOWLEDGMENTS

The work of the first and second authors was partially supported by Conacyt–México under grant CB–254329.

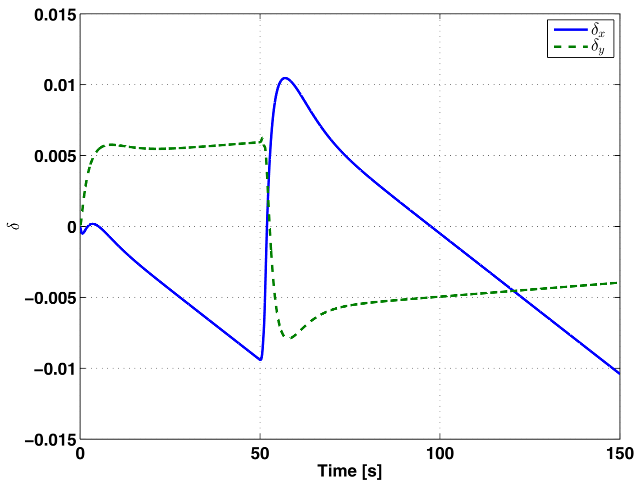

Fig. 11. Estimated disturbance $\eta_1 - \beta_1$.

REFERENCES

Astolfi, A. (1999). Exponential stabilization of a wheeled mobile robot via discontinuous control. *Journal of Dynamic Systems Measurement and Control*, 121, 121–125.

Astolfi, A., Karagiannis, D., and Ortega, R. (2007). *Nonlinear and adaptive control with applications*. Springer Science & Business Media.

Bhat, S.P. and Bernstein, D.S. (2000). A topological obstruction to continuous global stabilization of rotational motion and the unwinding phenomenon. *Systems & Control Letters*, 39(1), 63 – 70. doi: https://doi.org/10.1016/S0167-6911(99)00090-0.

Brockett, R.W. (1983). Asymptotic stability and feedback stabilization. In *Differential Geometric Control Theory*, 181–191. Birkhauser.

Buccieri, D., Perritaz, D., Mullhaupt, P., Jiang, Z.P., and Bonvin, D. (2009). Velocity-scheduling control for a unicycle mobile robot: Theory and experiments. *IEEE Transactions on Robotics*, 25(2), 451–458. doi: 10.1109/TRO.2009.2014494.

Chaturvedi, N.A., Sanyal, A.K., and McClamroch, N.H. (2011). Rigid-body attitude control. *IEEE Control Systems*, 31(3), 30–51.

Ginoya, D., Shendge, P., and Phadke, S. (2014). Sliding mode control for mismatched uncertain systems using an extended disturbance observer. *IEEE Transactions on Industrial Electronics*, 61(4), 1983–1992.

Jiang, Z.P. and Nijmeyer, H. (1997). Tracking control of mobile robots: A case study in backstepping*. *Automatica*, 33(7), 1393 – 1399. doi: https://doi.org/10.1016/S0005-1098(97)00055-1.

Khalil, H. (2002). *Nonlinear Systems*. Pearson Education. Prentice Hall. URL `https://books.google.com.mx/books?id=t_d1QgAACAAJ`.

Koditschek, D.E. (1989). The application of total energy as a Lyapunov function for mechanical control systems. *Contemporary Mathematics*, 97, 131.

Lee, T., Leok, M., and McClamroch, N.H. (2013). Nonlinear robust tracking control of a quadrotor UAV on SE(3). *Asian Journal of Control*, 15(2), 391–408.

Maghenem, M., Loría, A., and Panteley, E. (2016). Lyapunov-based formation-tracking control of nonholonomic systems under persistency of excitation. *IFAC-PapersOnLine*, 49(18), 404–409.

Maithripala, D. and Berg, J.M. (2015). An intrinsic pid controller for mechanical systems on lie groups. *Automatica*, 54, 189 – 200. doi: http://dx.doi.org/10.1016/j.automatica.2015.01.005.

McClamroch, H., Reyhanoglu, M., and Rehan, M. (2017). Knife-edge motion on a surface as a nonholonomic control problem. *IEEE Control Systems Letters*, 1(1), 26–31. doi:10.1109/LCSYS.2017.2700441.

Morin, P. and Samson, C. (2008). Motion control of wheeled mobile robots. In B. Siciliano and O. Khatib (eds.), *Springer Handbook of Robotics*, 799–826. Springer Berlin Heidelberg, Berlin, Heidelberg.

Oriolo, G., Luca, A.D., and Vendittelli, M. (2002). WMR control via dynamic feedback linearization: design, implementation, and experimental validation. *IEEE Transactions on Control Systems Technology*, 10(6), 835–852. doi:10.1109/TCST.2002.804116.

Rouchon, P., Fliess, M., Levine, J., and Martin, P. (1993). Flatness, motion planning and trailer systems. In *Proceedings of 32nd IEEE Conference on Decision and Control*, 2700–2705 vol.3. doi: 10.1109/CDC.1993.325686.

Sepulchre, R., Jankovic, M., and Kokotovic, P.V. (1997). *Constructive nonlinear control*. Springer Verlag.

Yang, J., Li, S., and Yu, X. (2013). Sliding-mode control for systems with mismatched uncertainties via a disturbance observer. *IEEE Transactions on Industrial Electronics*, 60(1), 160–169.

Zhang, Y., Hong, D., Chung, J.H., and Velinsky, S.A. (1998). Dynamic model based robust tracking control of a differentially steered wheeled mobile robot. In *Proceedings of the 1998 American Control Conference. ACC (IEEE Cat. No.98CH36207)*, volume 2, 850–855 vol.2. doi:10.1109/ACC.1998.703528.